

Modifications and Development of Stereo Correspondence Algorithms for the Passive Optoelectronic Rangefinder

Vladimir Cech¹ and Jiri Jevicky²

¹ Oprox, Inc.,
Kulkova 8, Brno, Czech Republic
cech-vladimir@volny.cz

² Department of Mathematics and Physics, University of Defence,
Kounicova 65, Brno, Czech Republic
jiri.jevicky@centrum.cz

Abstract: The principle of the passive optoelectronic rangefinder (POERF) is known since c. the second half of 1950s. Publications about research and development of POERF do not exist practically. Presumptive causes are presented in this article. We deal with POERF research and development since year 2003. The last fully functional demonstration model is from the year 2009. We present firstly its brief description with the aim to explain why modifications of commonly published stereo matching algorithms are necessary. We present a short characteristic of the algorithm that we use at present. In the second part of the article, we briefly specify problems pertinent to a suppression of the influence of foreground objects on the accuracy of ranges measurement. The third part indicates the basic approach to the evaluation of POERF accuracy with the aim to define convenient relative characteristics for the precision of estimates of the target range and the corresponding disparity.

Keywords: passive optoelectronic rangefinder (POERF), stereo matching algorithm, foreground object, measurement accuracy.

I. Introduction

The main goal of the article is to provide the basic information about POERF for specialist community and to arouse an interest in collaboration in the solving of modified algorithms suitable for applications in POERF.

The topographical coordinates of an object of interest (the target), which is represented by one contractual target point $T = (E, N, H)_T$, need to be determined indirectly in many cases that occur in practice, because an access to respectively the target and the target point T is disabled due to miscellaneous reasons at a given time.

Typical measured ranges interval for ground targets is from 200 to 4 000 m and for aerial or naval targets from 200 to 10 000 m or more.

Active rangefinders for measurement of longer distances of objects (targets), e.g. pulsed laser rangefinders (LRF), emit radiant energy, which conflicts with hygienic restrictions in many applications and sometimes with given radiant pollutions limitations, too. In security and military

applications there is a serious defect that the target can detect its irradiation. The use of POERF eliminates mentioned defects in full.

The passive optoelectronic rangefinder (POERF, Fig. 1, 2, 3) is a measurement device as well as a mechatronic system that measures geographic coordinates of objects (targets) selected by an operator in real time (in online mode). In the case of a moving object, it also automatically evaluates its velocity vector v_T and simultaneously extrapolates its trajectory.

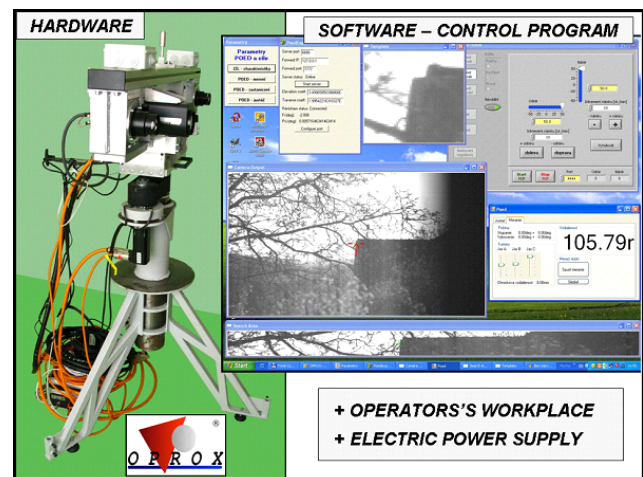


Figure 1. Passive optoelectronic rangefinder (POERF) – demonstration model 2009.

In general, the POERF continues to measure the UTM coordinates (Fig. 4) of a moving target with rate from 10 measurements per second and extrapolates its trajectory. All required information is sent to external users (clients) via the Internet in near-real-time whereas the communications protocol and the repetitive period (for example 1 s) are pre-concerted. The coordinates can be transformed to the coordinate system WGS 84 and sent to other systems – in accordance with the client's requirement.

The POERF is able to work in two modes: online and offline (processing of images saved in memory– e.g. on the hard disc). The offline mode enables to measure the distance of fleeting targets groups in time lag to approx. 30 seconds. The active rangefinders are not able to work in a similar mode.

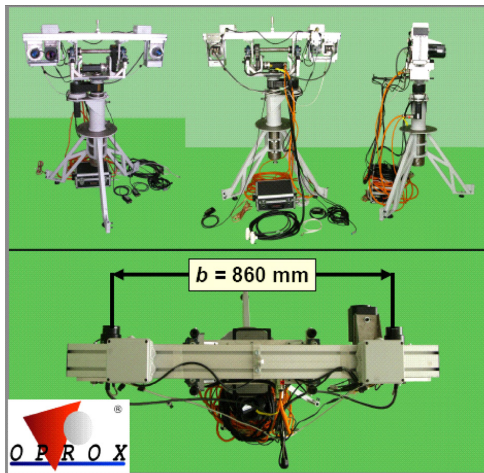


Figure 2. Photographs of the POERF hardware –demonstration model 2009.

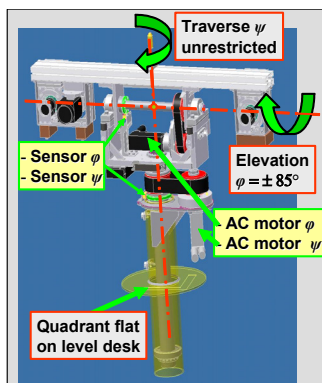


Figure 3. The kinematic structure of POERF.

Presumed users of the future system POERF are the police, security agencies (ISS – Integrated Security Systems, etc.) and armed forces (NATO NEC – the NATO Network Enabled Capability, etc.).

The POERF measurement principle is based on the evaluation of information from stereo-pair images obtained by the sighting (master) camera and the metering (slave) one. Their angles of view are relatively small and therefore a spotting camera with zoom is placed alongside the sighting camera – Fig. 1,2,3. This spotting camera is exploited by an operator for targets spotting. After operator’s steering the cameras towards a target, the images from the sighting camera serve to evaluate angle measured errors and to track the target automatically.

The patents of POERF components have been published since the end of 1950’s but there are no relevant publications dealing with the appropriate research and development results. We have not found out that similar device development is being carried out somewhere else. The problem itself consists particularly in users’ unshakable faith in limitless possibilities of laser rangefinders and probably in the industrial/trade/ national security directions.

The development was conditioned primarily by progress in the areas of digital cameras and by progress in miniature computers with ability to work in field conditions (target temperature limit from –40 to +50 °C, dusty environment, etc.) and to realize the image processing in the real-time (frame rate minimally 5 to 10 frames per second, ideally 25 to 30 fps).

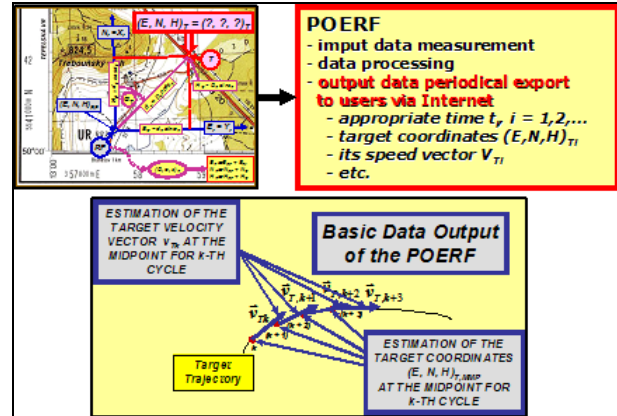


Figure 4. The principle of information processing by POERF.

Our development started initially on a department of Military Academy in Brno (since 2004 University of Defence) in the year 2001 in cooperation with the firm Oprox, Inc., Brno. The centre of the work was gradually transferred into Oprox that is practically the pivotal solver since the year 2006.

Similar principle is applied to focusing system of some cameras as well as mobile robots navigation/odometry systems. Measured distance range (Fig. 8) is within order one up to tens of meters, therefore the hardware and software concepts in these systems are different from concepts in the POERF system. Sufficient literature sources cover these problems.

A demonstration model of the POERF (Fig.1, 2, 3) was presented to the opponent committee of the Ministry of Industry and Trade of the Czech Republic within the final opponent proceeding in March 2009. The committee stated that POERF is fully functional and recommended continuing in its further research and development. The working range of measured distances is circa from 50 m to 1 000 m at the demonstration model.

From the system view, the POERF as a mechatronic system is composed of three main subsystems: the range channel, the direction channel and the system for evaluation of the target coordinates and for their extrapolation [1], [2] – Fig. 1, 2, 3.

The task of the range channel is on the one hand automatic recognition and tracking of the target which has been selected by the operator in semiautomatic regime and continuous measuring of its slant range D_T (circa 10 measurements per second at present, which is identical to cameras frame rate) and on the other hand the evaluation of angle measured errors (e_φ, e_ψ) that are transferred to input of the direction channel – Fig. 6.

The core of hardware consists of three digital cameras fixed through adjustable suspensions to the cameras beam: the sighting (master) camera, the metering (slave) camera and the spotting camera – Fig. 2, 3.

The algorithm for computation of estimate of a slant range D_T is based on solution of the telemetric triangle that lies in the triangulation plane (triangulation algorithms) – Fig. 5.

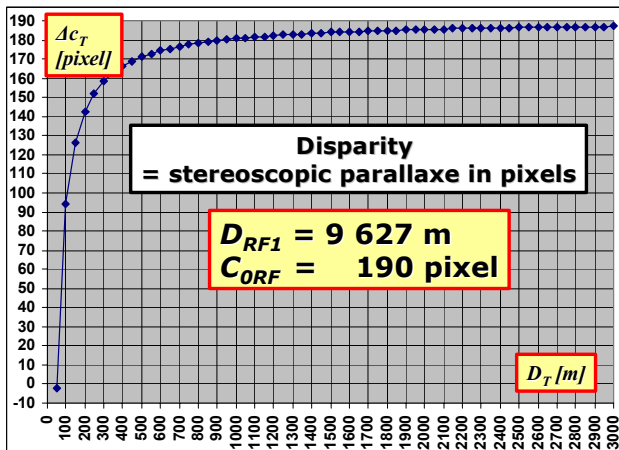


Figure 5. The triangulation dependence of the disparity Δc_T on the size of the slant range D_T , which is the function of two parameters D_{RF1} and C_{ORF} .

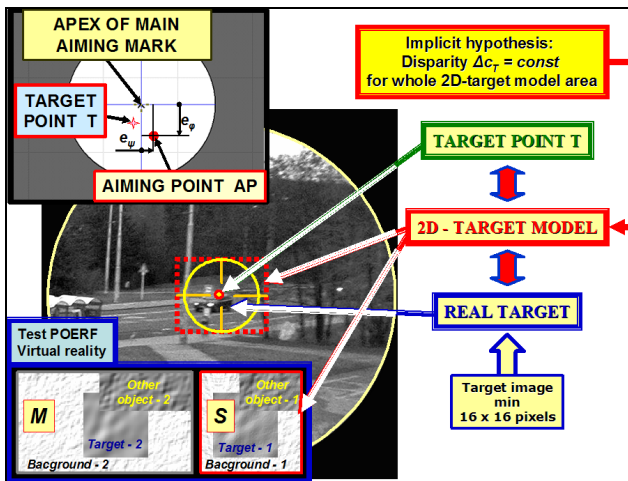


Figure 6. Relation among the image of the real target in the sighting camera, the target point T and 2D model of the target (the program Test POERF – see [3]).

The input data are ordinal numbers c_{T1} , c_{T2} of columns of matrix sensors in which images T'_1 , T'_2 of the target point T are projected. In particular, it is sufficient to determine their difference Δc_T (horizontal stereoscopic disparity) that is proportional to the appropriate parallaxic angle β . Therefore algorithms for computation of estimate of the difference Δc_T are crucial (the correspondence problem algorithms). We work with algorithms for an estimate of Δc_T , which involve the definition of 2D model of the target image (shortly “target model”). We use a rectangular target model for the present – Fig. 6. The positive value $d_T = C_{ORF} - \Delta c_T$ is usually regarded as the disparity [5]. The sign convention is elected so that $\Delta c_T \geq 0$ is valid for $D_T \geq D_\alpha$, where $D_\alpha = b/\tan \alpha_\Sigma$. The size of the convergence angle α_Σ (resp. α) is chosen with respect to the requirement that the measurement of the given minimal range D_{Tmin} of the target should be ensured. In our case $D_\alpha = c. 50$ m.

The basic equations for approximate computation of respectively the slant range and the appropriate disparity are

$$D_T \approx \frac{D_{RF1}}{C_{ORF} - \Delta c_T} \quad (1)$$

and

$$\Delta c_T \approx C_{ORF} - \frac{D_{RF1}}{D_T}, \quad (2)$$

where

$$\Delta c_T = c_{T2} - c_{T1},$$

$$D_{RF1} = \frac{b \cdot f_a}{\rho(c)},$$

$$C_{ORF} \approx \left(\frac{f_a}{\rho(c)} \right) \cdot \tan \alpha + \Delta c_{021} = \left(\frac{f_a}{\rho(c)} \right) \cdot \tan \alpha_\Sigma,$$

$$\Delta c_{021} = c_{20} - c_{10} = \Delta c_{021B} + \delta c_{021},$$

$$\Delta c_{021B} = c_{20B} - c_{10B},$$

$$\delta c_{021} = \delta c_{20} - \delta c_{10}.$$

The columns c_{20} , c_{10} determine the horizontal position of the principal points of autocollimation/projection of slave and master cameras [6]. If the target is in infinity (the Sun, the Moon, stars), then its disparity is just $\Delta c_T = C_{ORF}$. The rated value $C_{ORF} = 190.317$ pixels.

The size of C_{ORF} is determined by the mechanical – hardware adjustment (Δc_{021B}) in conjunction with the electronic – software one (δc_{021}).

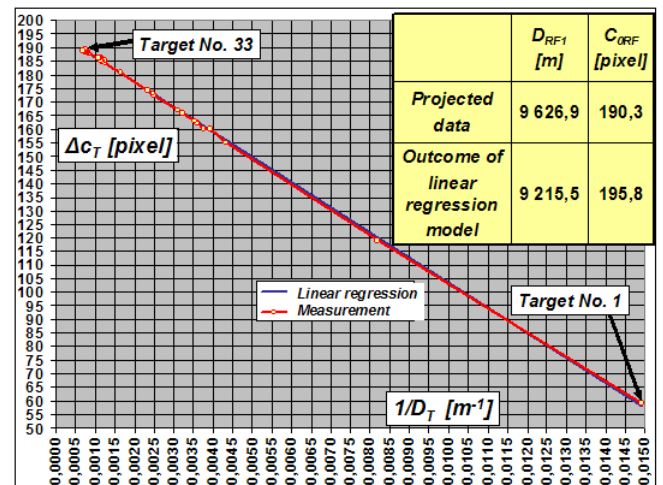


Figure 7. Summary of regression analysis results – the data file has contained approximately 50 thousands records (measurements of the range) [12].

The rangefinder power (constant) D_{RF1} is the basic characteristics of potential POERF accuracy. With increasing value of the power, the accuracy of measurement increases too. The rated power of POERF demonstration model is $D_{RF1} = 9 627$ m. The size of D_{RF1} depends on the width of rows of pixels $\rho(c) = \rho$, on the absolute value of the image focal length f_a and on the size of the base b (Fig. 2).

The actual values of constants D_{RF1} and C_{ORF} are determined during manufacturing and consecutively during operational adjustments. The adjustment is realized under utilization of several targets whose coordinates are known for high accuracy. The appropriate measurements are processed statistically with the use of the linear regression model (the component part of POERF software). For example, it was

determined for targets 1 to 33 from the Catalogue of Targets [3], [12] and for integer estimates of the disparities that $D_{RF1} = 9\,215.5$ m and $C_{ORF} = 195.767$ pixels (the correlation coefficient $r = -0.999\,725$) – Fig. 7.

The maximum computing speed is required primarily, in order that about from 10 to 30 range measurements per second are necessary in our applications (POERF). Therefore, we prefer simple (and hence very fast) algorithms. Random errors of measurements are compensated during statistical treatment of measurement results (extrapolation process).

The matching cost function $S(k)$ is used in the meantime (in general it is pixel-based matching costs function) – the sum of squared intensity differences SSD (or mean-squared error MSE) [3], [5], [10]. The computation of matching cost function $S(k)$ proceeds in two steps.

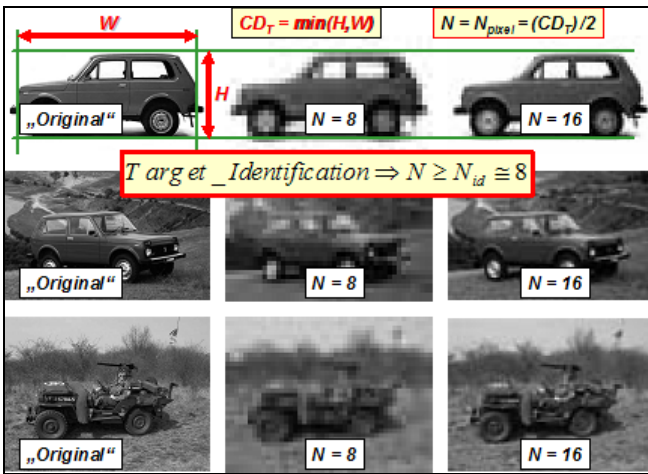


Figure 8. The impact of the target contrast towards the background and the number of sampling periods upon the possibility of its identification.

Firstly, its global minimum with one-pixel accuracy is calculated. In the second step, the global minimum is searched with sub-pixel accuracy while using the polynomial approximation. While using above-mentioned algorithms, it is always presumed that the same disparity $\Delta_{CT} = \text{const}$ is for all pixels of 2D target model – Fig. 6. This precondition is equivalent to the hypothesis that these pixels depict immediate neighborhood of the target point T representing the target and this neighborhood appertain to the target surface (more accurately all that is concerned the image T'_1 of this point and its neighborhood). These algorithms belong to the group referred to as local, fixed window based methods [5], [10].

It is necessary for the sake of reliable functioning of the system that the image of a target should be of size 16×16 pixels minimally, i.e. the number of sampling periods should be $N \geq 8$ (Fig. 6, 8) [1], [19].

Usual shapes of a target surface (e.g. balconies on a building facade, etc.) have only a little influence on the above-mentioned precondition violation (Fig. 12), because the range difference generated by them is usually less than 1 to 2 percent of the “average” target slant range D_T evaluated over the target surface represented by the 2D target model. Adduced precondition can be frequently satisfied by a suitable choice of size and location of the target model (i.e. by the aim of a convenient part of the target) – Fig. 6,12. The

choice is performed iteratively by the operator for the real POERF.

It is evident from the above that the choice of the position and the size of 2D target model is not a trivial operation and it is convenient to entrust a man with this activity. The operator introduces a priori and a posteriori information into the measurement process of respectively the disparity and the range of a target and this information can be only hardly (or not at all) obtained by the use of fully automatic algorithm.

Algorithms commonly published for the stereo correspondence problem solving are altogether fully automatic [5], [9], [20]–[24] – they use the information included in the given stereo pair images, eventually in several consecutive pairs (optical flow estimation). Therefore, it is possible to get inspired by these algorithms, but it is impossible to adopt them uncritically.

In conclusion it is necessary to state that these automatic algorithms are determined for solving the dense or sparse stereo-problems, whereas the POERF algorithms *estimate the disparity of the only point – the target point T*, but under complicated and dynamically varying conditions in the near-real-time.

Yet another difference exists between POERF and other devices exploiting stereo correspondence algorithms for the range measurement of objects.

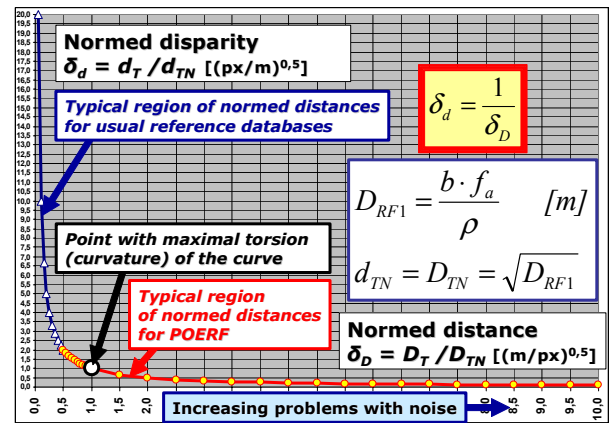


Figure 9. Dependence of the normed disparity δ_d on the normed target range δ_D .

These devices can have usually relatively large basis b (and consequently D_{RF1} , too) towards the extent of measured ranges, and so – from the view of triangulation algorithm – they work in the “left” branch of hyperbolic dependence between the range D_T of objects and corresponding disparity d_T ($d_T = C_{ORF} - \Delta_{CT}$) – Fig. 9. It means that small changes of D_T induce large changes of d_T (the system is very sensitive to changes of the range).

Such solution is not possible for POERF, because its sizes and weight would be unacceptable. Consequently, the POERF works in the “right” branch of mentioned dependence – Fig. 9. Thus, it is very insensitive to changes of the range, which produces exceptional demands on accurate estimate of the disparity Δ_{CT} . The situation is moreover complicated by the noise impact (see below).

II. Problems with Foreground Objects

In many cases it is inevitable that some pixels of the 2D target model record a rear (background) object or a front (foreground) object instead of the target. Simulation experiments with the program Test POERF [3] showed that farther objects have minimal adverse impact on the accuracy of the range measurement, contrary to nearer objects that induce considerably large errors in the measurement of the target range. From the problem merits, these errors are random blunders. Their greatness depends on the mutual position of the foreground object and the target – Fig. 10. This finding has been also verified in computational experiments by the help of the program RAWdis [3]. The foreground object usually causes that the set of pixels of the 2D target model is not connected (it is the union of several connected subsets). In many situations, the number of “effective” pixels in this set can be less than it matches with the evaluation of the image from the sighting camera only and it is the source of mentioned problems.

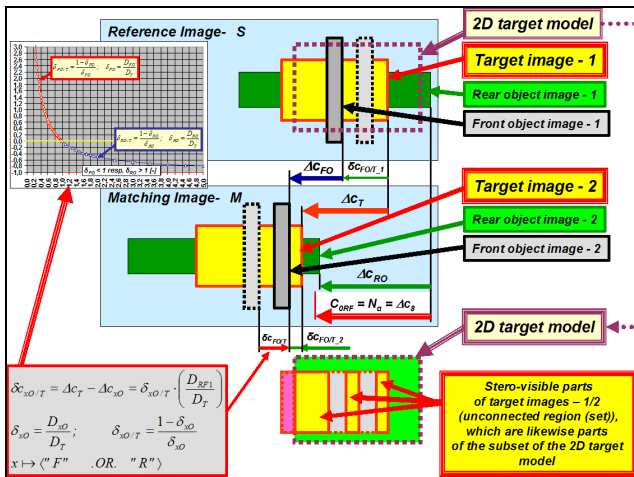


Figure 10. The front object influence on the distortion of results of the target range measurement.

As it is obvious, this case is a special implication of the well-known problem referred to as “occluded areas” [7], [9], [20].

If any object moves relatively towards the POERF at another velocity than objects in the foreground, then algorithms utilizing computed optical flows can be used for discrimination of pixels which represent near objects [21], [22], [23], [24].

If objects do not move relatively one another, then the situation is considerably complicated as it is shown hereinafter.

The concrete example of described phenomenon is introduced in the Fig. 11. The effect evinces on the graph deformation of the matching cost function $S(k)$ in a neighborhood of its global minimum. The graph “Target” ($D_T = 245$ m) corresponds to the choice of 2D target model, where all its pixels depict surface of the target – the building (accurately measured range of the target) and the graph “Light pole” ($D_F = 178$ m) corresponds analogically to the choice, where all pixels depict surface of the foreground object (accurately measured range of this object). Each of these

graphs has the only one “decided” local minimum which is simultaneously the global minimum. The graph “Wrong estimation” ($D_{Twrong} = 193$ m) corresponds to so chosen position and size of the 2D target model that a part of pixels displays an image of the target and the rest displays an image of the foreground object. The graph has two local minima which are shifted against the positions of minima of two basic graphs. Besides, a concrete random choice of the position and the size of 2D target model decide which of two local minima will be the global minimum. In reality, the structure of disconnected set of “effective” pixels can be considerably complicated, e.g. due to branches of trees – Fig. 11.

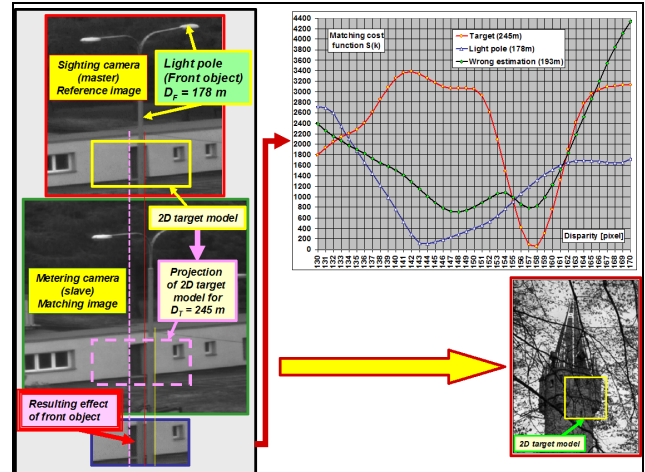


Figure 11. The example of a front object influence on the creation of disconnected set of “effective” pixels on the 2D target model displaying the surface of the target No. 4 – a building [2], simulation results from the program RAWdis and the second example of a front object influence (branches of trees – cluttered foreground).

At present we work on algorithms that suppress influences of foreground objects and that simultaneously work in the iterative mode – a dialog with the operator – such as the algorithms SIOX [4]. It is concerned about a special application of algorithms for foreground extraction from 2D target model [4], [7], [8], [22], [23]. The size of the 2D target model is up to 64×64 pixels in reality, i.e. up to c. 4096 pixels. This attribute accelerates calculations substantially, but many algorithms are disqualified simultaneously. The fact that foreground objects belong to “cluttered foreground” category needs to be considered too [7] – Fig. 1, 11.

The functionality of algorithms will be verified by the help of advanced versions of programs RAWdis (real scenes) and Test POERF (virtual scenes).

At the present, we have developed a generator of “twiggy”, where all requisite parameters can be chosen and so we can probe the effectiveness of algorithms for suppression of influence of foreground objects (we accurately know ground-truth disparity map). In the Figure 12 there are unmodified images of a building (the program RAWdis). In the Figure 13 there is an example of generated “twiggy” and its insertion (in chosen ranges) into the original images. The effect of “twiggy” is obvious from the example of the course of the matching cost function $S(k)$ – Fig. 14. A description of used algorithms transcends the scope of this article.

III. Problems with Noise

Errors in a scene record (distortion of its image in the shot) are on the one hand gross and systematic, and on the other random (spatial noise). The gross errors are removed by the procedure referred to as „pixel mapping“. The systematic errors are eliminated with using the average dark frame and the average flat field frame [3]. The residual value of standard deviation σ_{SN} characterizes the random error component denoted as the spatial noise [15, 16].

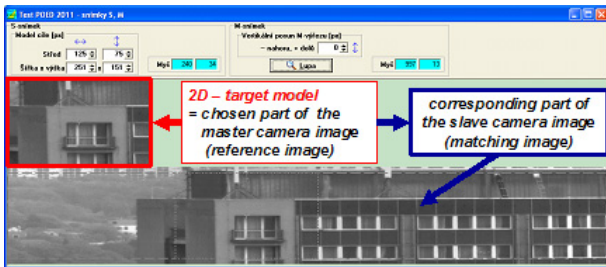


Figure 12. Original stereo-pair images (a window of the program RAWdis), Target No. 10/3 ($D_{T0} = 320,6$ m) of Catalogue of Targets.

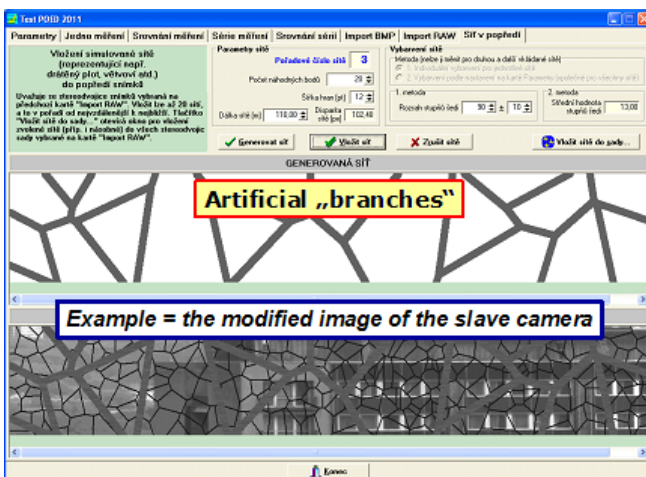


Figure 13. The sample of a “twiggery” generation and a modified image from the slave camera (program RAWdis).

At laboratory conditions, two quantities are used to its characterization: dark signal non-uniformity (DSNU) and photo response non-uniformity (PRNU). These quantities characterize the noise properties of respectively the digital matrix sensor (DMS) and the whole record chain. This spatial noise component can be suppressed by digital matrix sensor cooling, in contrast with the noise component which is determined by the atmosphere attenuation [1], [18] and turbulence level [1]. In the course of a scene record for use in measurement of a target range, the atmosphere attenuation and turbulence – as a dynamic process running in the transmission channel – influences the size of the spatial noise significantly. Its share in the spatial noise cannot be separated from the share of the own recording device only by the realization of special experiments.

The real range of the demonstration model POERF is given by the accuracy of finding the disparity (standard deviation σ_C [pixel], resp. $\sigma(c) = \sigma_C \cdot \rho(c)$ [m]), and by the value of the power constant D_{RF1} .

The accuracy of the target range measurement depends not only on properties of the own rangefinder, but on the whole system composed from the rangefinder, the atmosphere [1], [18], a target, a target’s surroundings, an operator and a lighting. Dependability and accuracy of the range measurement is characterized especially with the use of the (sample) standard deviation of measured range σ_{DT} (resp. s_{TM}) and the (sample) relative standard deviation of measured range (D_{T0} is the true range, which is a priori known)

$$\sigma_{DR} = \frac{\sigma_{DT}}{D_{T0}}, \text{ resp. } s_{DR} = \frac{s_{TM}}{D_{Taver}}. \quad (3)$$

Instead of the (sample) standard deviations σ (resp. s), corresponding probable errors E (resp. e) are often used. It is valid for normal distribution $E = 0.6745 \cdot \sigma$. The value of the relative probable error E_{DR} is usually required less than 2 to 4% in a requisite interval of ranges under good conditions – day conditions and meteorological visibility s_M (or MOR – meteorological optical range) over 10 km.

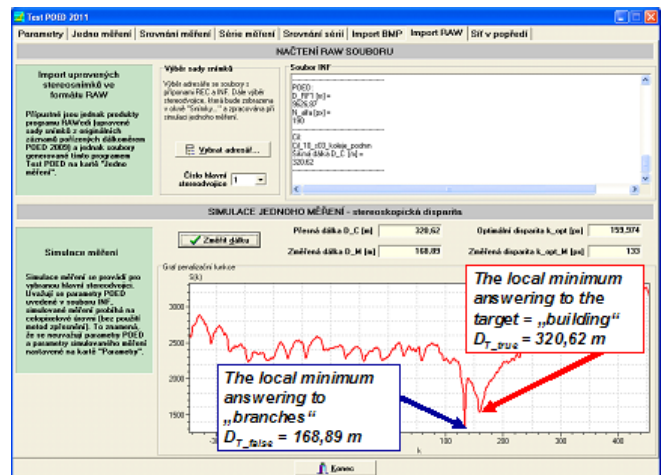


Figure 14. The example of the course of the matching cost function $S(k)$ (program RAWdis).

The parameter that influences the size D_{RF1} is the length of the base b (see the commentary to the Figure 9). Its size is selected with respect to the demand for accomplishment of requisite size $D_{T0} = D_{Tmax}$ – the maximum working range, in which the relative size of the probable error E_{DR} of the range measurement attains the given size, e.g. 3% – Fig. 17. The size of the base b depends simultaneously on the size of the standard deviation $\sigma(c)$ (resp. σ_C) of determination of the disparity Δc_T corresponding to the range D_{Tmax} ,

$$\sigma_C = \frac{\sigma(c)}{\rho(c)} = \sigma_{C0} \cdot \sigma_{CR}. \quad (4)$$

As its basic (standardizing) value σ_{C0} can be elected the standard deviation originating always at integer finding the value of the disparity Δc_T as an unrecoverable discretization (quantizing) noise with the uniform distribution on the interval of the length just one pixel – Fig. 15, 17. Then it is

$$\sigma_{C0} = \frac{1}{\sqrt{12}} \approx 0.2887. \quad (5)$$

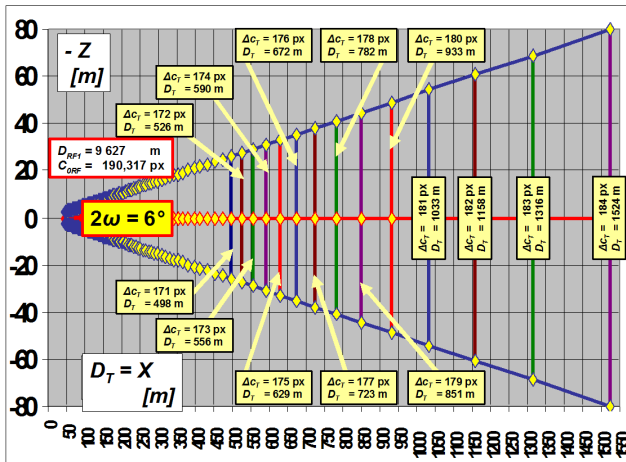


Figure 15. The implication of disparity estimate $\Delta c_T = i$ with one-pixel accuracy (i is an integer, $i \leq i_{\max} < C_{\text{ORF}}$) is the nonlinear discretization of measured target ranges D_{T_i} .

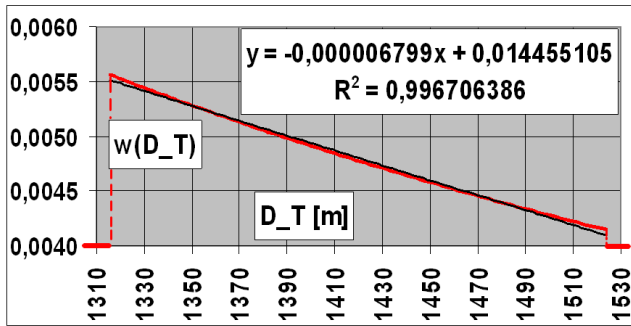


Figure 16. The probability density $w(D_T)$ as the function of the range D_T for the interval that corresponds with the disparity interval (in pixels, see the Figure 15) $\Delta c_T \in (183, 184)$.

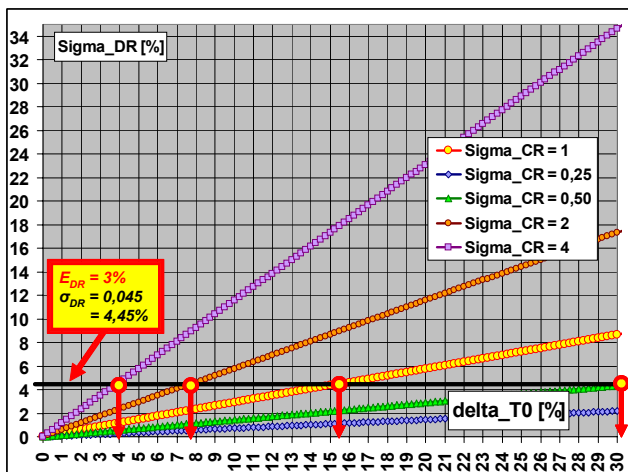


Figure 17. The main relations for estimate of POERF accuracy.

Instead of values σ_c , their relative values σ_{CR} can be used so. The value σ_c (resp. σ_{CR}) is the quality indicator for appropriate hardware and software of the POERF, especially for algorithms for estimates of sizes of the disparity Δc_T under given conditions (meteorological visibility, atmospheric turbulence, exposure time, aperture ratio, motion blur, etc.). If the value of σ_{CR} increases twice, then it is necessary to

elongate the base b also twice with a view to preserve the requisite value D_{Tmax} . Whence it follows that the quality of hardware and software immediately influences the POERF sizes and mass that are directly proportional to the size of base b .

The value of σ_{CR} is equal approximately to 2 for the first 33 targets from the Catalogue of Targets and this value is taken as the residual error of linear regression for the determination of parameters D_{RF1} and C_{ORF} – Fig. 7, 18, 19. Then $\sigma_c = 0.2887$ $\sigma_{\text{CR}} = 0.577$ px and $\sigma(c) = 3.87$ μm ($\rho(c) = 6.7$ μm).

The following formula can be used to convert σ_c to σ_{DR}

$$\sigma_{\text{DR}} \approx \left(\frac{D_{\text{T0}}}{D_{\text{RF1}}} \right) \cdot \sigma_c = \sigma_{\text{DR0}} \cdot \sigma_{\text{CR}}, \quad (6)$$

where

$$\sigma_{\text{DR0}} = \delta_{\text{T0}} \cdot \sigma_{c0} \approx 0.2887 \cdot \delta_{\text{T0}}, \quad \delta_{\text{T0}} = \frac{D_{\text{T0}}}{D_{\text{RF1}}}.$$

This formula is approximate – Fig. 17. It is derived under condition of the Taylor series expansion of the function $D_T(\Delta c_T)$ – Fig. 5 – in the operating point. A comparison with exact relations shows that the relative error of the formula is less than 1% for $c = \Delta c_T / C_{\text{ORF}}$ up to 0.97 and for c up to 0.99 does not exceed 30%.

We will use the Figure 16 to clarify foregoing findings. Owing to the incidence of many influences, the computed estimates of the disparity Δc_T are burdened with random errors. In the situation, when we have no a priori information, there are possible different presumptions about the distribution of the random variable Δc_T . For simplicity, we will assume the uniform distribution on some interval $\langle d_L, d_U \rangle$. This presumption is fully satisfactory, for example, in the investigation of the predominant influence of the discretization error.

The corresponding estimate D_{TM} of the slant range D_T , computed by the use of the formula (1), is the function of one random variable – the disparity Δc_T . The probability density function $w(D_T)$ of the random variable D_{TM} is of hyperbolic type on the interval of ranges with the endpoints that corresponds to the disparity values d_L, d_U . In the Figure 16, there is the graph of the probability density function of the random variable D_{TM} supposing the uniform distribution of the disparity Δc_T on the interval $\langle 182, 183 \rangle$, and the graph of linear approximation of this density function, too.

For the exact courses and also for the linear approximation, the values of the standard deviations σ_D were computed, and consecutively of the relative standard deviations σ_{DR} , too. These values were compared with values, which were computed using the above simplified formulas, and it was found – from the view of practical usage – insignificant differences for values c up to 0.97, which have an importance for the practice.

Our nearest aim is to find the real values of parameters of the spatial noise PSD from the images filed into the Catalogue of Targets [3] and also from the images taken in days with higher level of the atmosphere turbulence.

In the following step – with the use of simulations programs Test POERF and RAWdis – we plan to develop and

to test fast algorithms for the suppression influence of the spatial noise on the disparity determination with sub pixel accuracy (the system must work in real time with frame rate c. 30 fps).

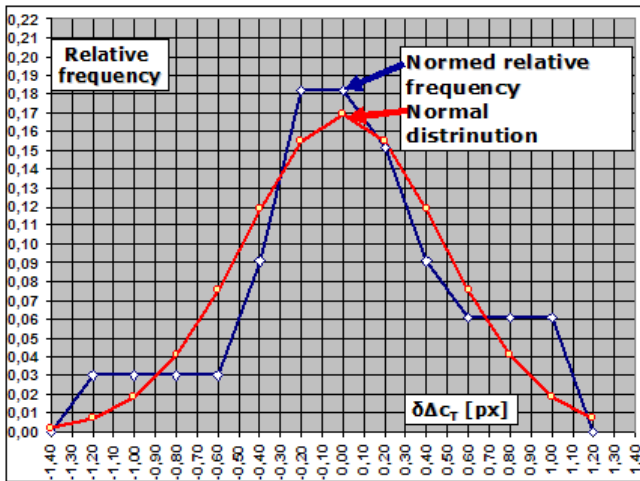


Figure 18. Distribution of residual errors (linear regression for the determination of parameters D_{RF1} and C_{ORF} – Fig. 7). Every point in the graph represents the mean from c. 1500 measurements [12].

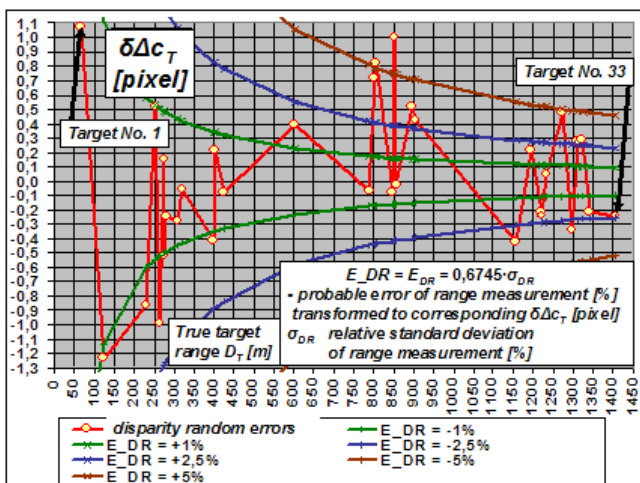


Figure 19. Dependence of residual errors upon ranges of targets (linear regression for the determination of parameters D_{RF1} and C_{ORF} – Fig. 7). Every point in the graph represents the mean from c. 1500 measurements [12].

Above mentioned values $\sigma_{CR} = c. 2 [-]$, $\sigma_C = 0.577 \text{ px}$ and $\sigma(c) = 3.87 \mu\text{m}$ are the first estimates of POERF accuracy, which were published [11]. We did not succeed in finding analogous results in available resources. In this regard it can be taken as a reference standard with which can be compared newly developed POERF systems and also existing coincidence and stereoscopic rangefinders.

We introduce an example of comparison with stereoscopic rangefinder DS-1 (Fig. 20). This system has similar parameters as the demonstration model of POERF.

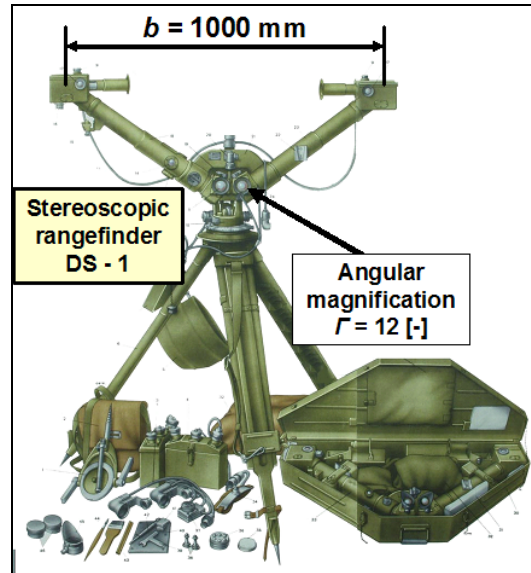


Fig. 20 Stereoscopic Rangefinder DS-1 (USSR).

The primary difficulty in comparison of coincidence and stereoscopic rangefinders with POERF consists in two circumstances:

- a) Various sources adduce different characteristics of human visual system [14],[17]. For calculations, it is necessary to elect at least focal length of human eye f_H . We elect $f_H = 17.05 \text{ mm}$, as the valid value for the theoretic eye [17]. According to other authors it can be chosen $f_H = 14.3$ to 16.5 mm in accordance with eye accommodation [17], but e.g. also 18.5 mm . A deeper analysis needs furthermore characteristic sizes of the cone $\rho_{H\text{foveola}}$ in the foveola (fovea centralis in the macula of the retina) – from our view they are equivalent sizes of special pixels of the human eye. Various authors indicate values in the range from 0.5 to $4 \mu\text{m}$. For possible analysis e.g. the value $\rho_{H\text{foveola}} = c. 2 \mu\text{m}$ can be chosen [17].

- b) Several methods exist for evaluation of visual acuity. In our case, it is necessary to study hyperacuity, especially vernier acuity and precision of (lateral) stereopsis (on axis). The problem consists in the fact that measurement methodology determines values [14],[17], which can not be simply convert to corresponding standard deviations $\sigma(c) [\mu\text{m}]$, which need to be in use in our computations. In the textbook [13] there are determined values for consistency and precision that are valid for the rangefinder DS-1 and for measurement of stationary targets. Because it is valid that $f_a = \Gamma \cdot f_H = 12 \cdot 0.01705 = 0.210 \text{ m}$ and $b = 1 \text{ m}$, the corresponding values for $\sigma(c)$ can be determined with using above mentioned relations. The parameter consistency is $\sigma_c(c) = c. 2.18 \mu\text{m}$ and the parameter precision is $\sigma_p(c) = c. 1.87 \mu\text{m}$, and so it is valid $\sigma_d(c) = c. 2.87 \mu\text{m}$ for the resultant accuracy. The values hold true under relatively good light conditions. At twilight namely the function of the cones is minimal and perception is based on the activity of rods, which are not placed at all in the area of foveola, and so the operator is losing the ability to measure a range accurately (visual acuity declines rapidly) in contrast to the POERF.

If the value $\sigma(c) = c. 3.87 \mu\text{m}$ founded for POERF is interpreted as a characteristic of consistency, i.e.

$\sigma(c) = \sigma_c(c) = c \cdot 3.87 \mu\text{m}$, then POERF (its hardware and software) has 1.78 times worse parameters than DS-1.

The same value $\sigma(c) = c \cdot 3.87 \mu\text{m}$ can be interpreted as a characteristic of the resultant accuracy, too. This variant is more probable with regard to the definition of residual errors of measurement, i.e. $\sigma(c) = \sigma_a(c) = c \cdot 3.87 \mu\text{m}$. Then POERF (its hardware and software) has 1.35 times worse parameters than DS-1.

Three ways lead to equalization of POERF accuracy parameters to accuracy of DS-1:

- A modification of hardware so that the actual value $(b \cdot f_a) = 0.0645 \text{ m}^2$ will increase respectively 1.35 and 1.78 times. It can be achieved preferably by an extension of the base respectively 1.35 and 1.78 times, i.e. to 1.16 m or 1.53 m. Consequently, the sizes of POERF will enlarge and partially also its weight. Possible extension of the focal length f_a causes reducing of angles of view with disadvantageous impacts on POERF functioning in the offline mode.
- It is needful to work intensively on the software development, in the first place on development of the stereo correspondence algorithm. The objective is to decrease the actual value $\sigma(c) = 3.87 \mu\text{m}$ respectively 1.35 and 1.78 times, accordingly to the value $c \cdot 2.87 \mu\text{m}$ or $c \cdot 2.18 \mu\text{m}$. If the actual pixel size will be preserve, then it is necessary to decrease the actual value $\sigma_{CR} = c \cdot 2$ [-] on the value $c \cdot 1.5$ resp. $c \cdot 1.12$.
- The requisite improvement of POERF parameters can be also achieved by a combination of modifications of hardware and software.

Last, it can be observed:

- The POERF parameters refer to the first fully functional demonstration model and so it can be expected that the next POERF development will produce betterment of its parameters.
- It is possible to accept a worse accuracy of the POERF towards the DS-1 partially, because the POERF is fully functional at twilight and also at moon night, whereas DS-1, owing to properties of the human visual system, is practically non-functional without powerful artificial lighting of the scene (terrain).
- Introduced comparison is an appeal for improvement of software and especially the stereo correspondence algorithms convenient for POERF. It is necessary to accent again, as it follows from above, that commonly published stereo matching algorithms can not be applied without their radical correction – e.g. [4], [7]–[9], [19]–[24].

IV. Conclusion

At present, we are finishing the new versions of simulation programs RAWdis (for real scenes) and Test POERF (for virtual scenes) with implemented tools for the suppression of foreground objects influences on the accuracy of ranges measurement.

As it is evident from the foregoing text, the range of tasks in the POERF software development is very extensive. Therefore, we welcome proposals for cooperation.

V. Acknowledgements

This work has originated under the support of financial means from the industrial research project of the Ministry of Industry and Trade of the Czech Republic – project code FR – TI 1/195: "Research and development of technologies for intelligent optical tracking systems".

VI. References

- [1] V. Cech and J. Jevicky, "Research and development of the passive optoelectronic rangefinder". In *Optoelectronic Devices and Properties*, Oleg Sergiyenko (Ed.), InTech 2011, pp. 323–348, ISBN 978-953-307-204-3.
- [2] V. Cech, J. Jevicky, and M. Pancik, "Demonstration Model of Passive Optoelectronic Rangefinder". In *Proceedings of the 8th International Conference Mechatronics 2009 „Recent Advances in Mechatronics 2008-2009“*. Editors: Brezina, T. – Jablonski, R., Luhacovice, November 18–20, 2009, Springer-Verlag Berlin Heidelberg 2009, pp. 79 - 84, ISBN 978-3-642-05021-3.
- [3] V. Cech and J. Jevicky, "Development of the Simulation Software Package Test POERF RAW". In *Proceedings of the 7th EUROSIM Congress on Modelling and Simulation*. Prague, Czech Republic, 2010. Vol. 1: Book of Abstracts, p. 1. ISBN 978-80-01-04588-6. Vol. 2. Full Papers (CD), 10 pages, ISBN 978-80-01-04589-3.
- [4] G. Friedland, K. Jantz, T. Lentz, and R. Rojas, "Extending the SIOX Algorithm: Alternative Clustering Methods, Sub-pixel Accurate Object Extraction from Still Images, and Generic Video Segmentation". Free University of Berlin, Department of Computer Science, Technical Report B-06-06, January 2006.
- [5] H. Hirschmüller and D. Scharstein, "Evaluation of cost functions for stereo matching". In *IEEE Computer Society Conference on Computer Vision and Pattern Recognition (CVPR 2007)*, Minneapolis, MN, 2007, ISBN 1-4244-1180-7.
- [6] K. Kraus, "Photogrammetry," Volume 1 – Fundamentals and Standard Processes, Dümmler, Bonn, 1999, 4th edition, ISBN 3-427-78684-6.
- [7] B. Nagarajan and P. Balasubramanie, "Cluttered Background Removal in Static Images with Mild Occlusions," *International Journal of Recent Trends in Engineering*, Vol. 1, No. 2, May 2009, pp. 134–136.
- [8] Piccardi, M. "Background Subtraction techniques: a review," *Proc. IEEE. SMC*, Vol. 4, 2004, pp. 3099–3104.
- [9] C. L. Zitnick and T. Kanade, "A Cooperative Algorithms for Stereo Matching and Occlusion Detection," *IEEE Transactions on Pattern Analysis and Machine Intelligence*, Vol. 22, No. 7, July 2000, pp. 675–684, ISSN 0162-8828.
- [10] D. Scharstein and R. Szelisky, "A Taxonomy and Evaluation of Dense Two-Frame Stereo Correspondence Algorithms," *International Journal of Computer Vision*, Vol. 47 (1-3), April 2002, pp. 7-42, ISSN 0920-5691.
- [11] V. Cech and J. Jevicky, "Modification of the Stereo Correspondence Problem for Passive Optoelectronic Rangefinder". In *Proceedings of the 2011 International*

- Conference of Soft Computing and Pattern Recognition (SoCPaR)*, Dalian, China, 2011, pp. 184-189. ISBN 978-1-4577-1194-7.
- [12] V. Cech and J. Jevicky: "The Catalogue of Stereo-Pairs Images as a Simulation Development Tool". In *Proceedings of UKSim 13th International Conference on Computer Modelling and Simulation EUROSIM/UKSim2011*, Cambridge, UK, 2011, p. 325-330. ISBN 978-0-7695-4376-5.
- [13] Composite authors, "Fire and Fire Control of the Field Artillery". Textbook ; Del – 55 – 26. Ministry of Defence of the Czechoslovak Socialistic Republic, Prague 1981, 856 p.
- [14] P. G. J. Barten, "Contrast sensitivity of the human eye and its effects on image quality". SPIE 1999.
- [15] F. Benzarti and H. Amiri, "Blind Photographic Images Restoration with Discontinuities Preservation", *International Journal of Computer Information Systems and Industrial Management Applications*, Volume 4, pp. 609-618, 2012, ISSN 2150 - 7988
- [16] A. Histace and D. Rousseau, "Useful Noise Effect for Nonlinear PDE Based Restoration of Scalar Images" *International Journal of Computer Information Systems and Industrial Management Applications*, Volume 4, pp. 411-419, 2012, ISSN 2150 - 7988
- [17] J. Stanek, "Visual Photometry and Physiological Optics". Inset of journal "Precision Mechanics and Optics". Prague. Czech Republic, SNTL 1980, 152 p. [In Czech]
- [18] A. Ch. Aponso and N. Krishnarajah, "Review on State of Art Image Enhancement and Restoration Methods for a Vision Based Driver Assistance System with De-weathering". In *Proceedings of the 2011 International Conference of Soft Computing and Pattern Recognition (SoCPaR)*, Dalian, China, 2011, pp. 135 – 139.
- [19] Y. Kang, G. Wang and J. Hu, "A Mean Shift Based Small Target Tracking Algorithm in Colored Video". In *Proceedings of the 2011 International Conference of Soft Computing and Pattern Recognition (SoCPaR)*, Dalian, China, 2011, pp. 407 – 412.
- [20] W. Zhu, D. Lu, Ch. Diao and J. Huang, "Variational Stereo Matching with Left Right Consistency Constraint". In *Proceedings of the 2011 International Conference of Soft Computing and Pattern Recognition (SoCPaR)*, Dalian, China, 2011, pp. 222 – 226.
- [21] X. Liu, B. Dia and H. He, "Real-time Object Segmentation for Visual Object Detection in Dynamic Scenes". In *Proceedings of the 2011 International Conference of Soft Computing and Pattern Recognition (SoCPaR)*, Dalian, China, 2011, pp. 423–428.
- [22] L. Yang, Y. Guo, X. Wu and X. Wang, A "New Video Segmentation Approach: GrabCut in Local Window". In *Proceedings of the 2011 International Conference of Soft Computing and Pattern Recognition (SoCPaR)*, Dalian, China, 2011, pp. 419 – 422.
- [23] M. Wan, X. Qin and L. He, "Background Modeling using Mixture of Gaussians and Laplacian Pyramid Decomposition". In *Proceedings of the 2011 International Conference of Soft Computing and Pattern Recognition (SoCPaR)*, Dalian, China, 2011, pp. 33 – 38.
- [24] T. Hong, W. Lixia and D. Xiaoqing, "Pedestrian Detection Based on Merget Cascade Clasifier". In *Proceedings of the 2011 International Conference of Soft Computing and Pattern Recognition (SoCPaR)*, Dalian, China, 2011, pp. 237 – 241.

Author Biographies



Vladimir CECH was born in Pisek, Czech Republic, in 1953. In 1977 he graduated from the Brno Military Academy – Dipl. Eng - mechanics; Ph.D. - the Brno Military Academy 1983 in the field: the Military Technology – the Weapons and Ammunition , associate professor - the Brno Military Academy 1989; habilitation in the field: the Military Technology – the Weapons and Ammunition - the Brno Military Academy 1993. The last military rank: Colonel of the General Staff.

Senior manager; since 1983 – teacher at the Brno Military Academy; since 1991 – head of the Weapon systems department ; since 1994 - Vice-Rector - Director of the Studies - at the Military Academy in Brno – deputy of the statutory body – Rector/Commandant, since 1997 - Vice-Rector - Director of the Development of the University - at the Military Academy in Brno - deputy of the statutory body – Rector/Commandant, since 1998 - General Director of the Personnel and Social Policy Department of CR DoD, since 2002 - Management and Consultancy Services in the field the Mechatronics, Weapons Systems, Education and Personnel Systems. Since 2003 he collaborates with the company OPROX, a.s. (Inc.), Brno, Czech Republic, in area of the research and development of the Passive optoelectronic Rangefinder (POERF).

Since 2011 University of Trencin, Faculty of Special Technologies, department of Automatization, Robotics and Informatics, Slovak Republic.

Founding member of International Ballistics Society.



Jiri JEVICKY was born in Brno, Czech Republic, in 1949. In 1972 he graduated from Faculty of Science, Masaryk University in Brno, in the field of Mathematics, specialization: Applied Mathematics. He received Ph.D. degree from Military Academy in Brno (MA) in 1982 in the field of Engineering Cybernetics; he vindicated dissertation work "Mathematical Model of Hierarchical Control System".

Since 1973 he works in Department of Mathematics in MA, first as lecturer and since 1989 as associate professor. From the year 2000 to 2005 he was the head of Department of Mathematics. Since September 2004 is the MA renamed to University of Defence in Brno.

Since 2003 he collaborates with the company OPROX, a.s. (Inc.), Brno, Czech Republic, in area of the research and development of the Passive optoelectronic Rangefinder (POERF).